CME LIVE OPEN ACCESS

Journal of
Earth & Environmental Waste Management

Research Article ISSN: 3065-8799

Assessment of the Effects of Land use Land Cover Change on Water Balance Components in the Upper Erer Subbasin, Wabishebele Basin, Ethiopia

Bedasa Abrahim Mummed* and Yilma Seleshi

Addis Ababa University, Addis Ababa Institute of Technology, Ethiopia.

Corresponding Author: Bedasa Abrahim Mummed, Addis Ababa University, Addis Ababa Institute of Technology, Ethiopia.

Received: 2024 Dec 14 **Accepted:** 2025 Jan 06 **Published:** 2025 Jan 23

Abstract

Land use change has a vital role in disturbing the hydrological response and assessing the LULC change and its impacts on the hydrological response is required for efficient water resource planning. The extent of LULC changes at the local level was uncertain and how the hydrological conditions were affected by LULC changes locally was a challenge. This study focused to assess the LULC change and its impacts on the hydrological components in the upper Erer sub basin using SWAT model from 2001 to 2020. The LULC change indicated that agricultural lands (3.97%) forest lands (3.99 %), and water bodies (0.60 %) were decreased and settlements (2.30%), shrub land (3.07%) and bare land (3.19) were increased. The model was calibrated and validated using monthly flow data indicates the performance was within satisfactory range of PBIAS ≤ (±25%), R2 > 0.8 and NSE > 0.5. The surface runoff, ground water flow, and water yields were increased by 6.03, 8.22, and 10.39 %, respectively. While, evapotranspiration was decreased by 3.34%. In this study, the change in LULC has significantly affected the hydrological component of the sub basin. This implies the implementation of adaptation strategies for sustainable water resource management in the region.

Keywords: Surface Runoff, Evapotranspiration, Lateral Flow, Land Use Land Cover Change, Manual Calibration

Highlights

- Using the Landsat image the image classification is performed.
- The study employed SWAT model for water balance component assessment.
- The land use land cover change was used to detect the surface runoff, potential and actual evapotranspiration, water yields, groundwater and lateral flow effects were evaluated in this study.

Graphical Abstract

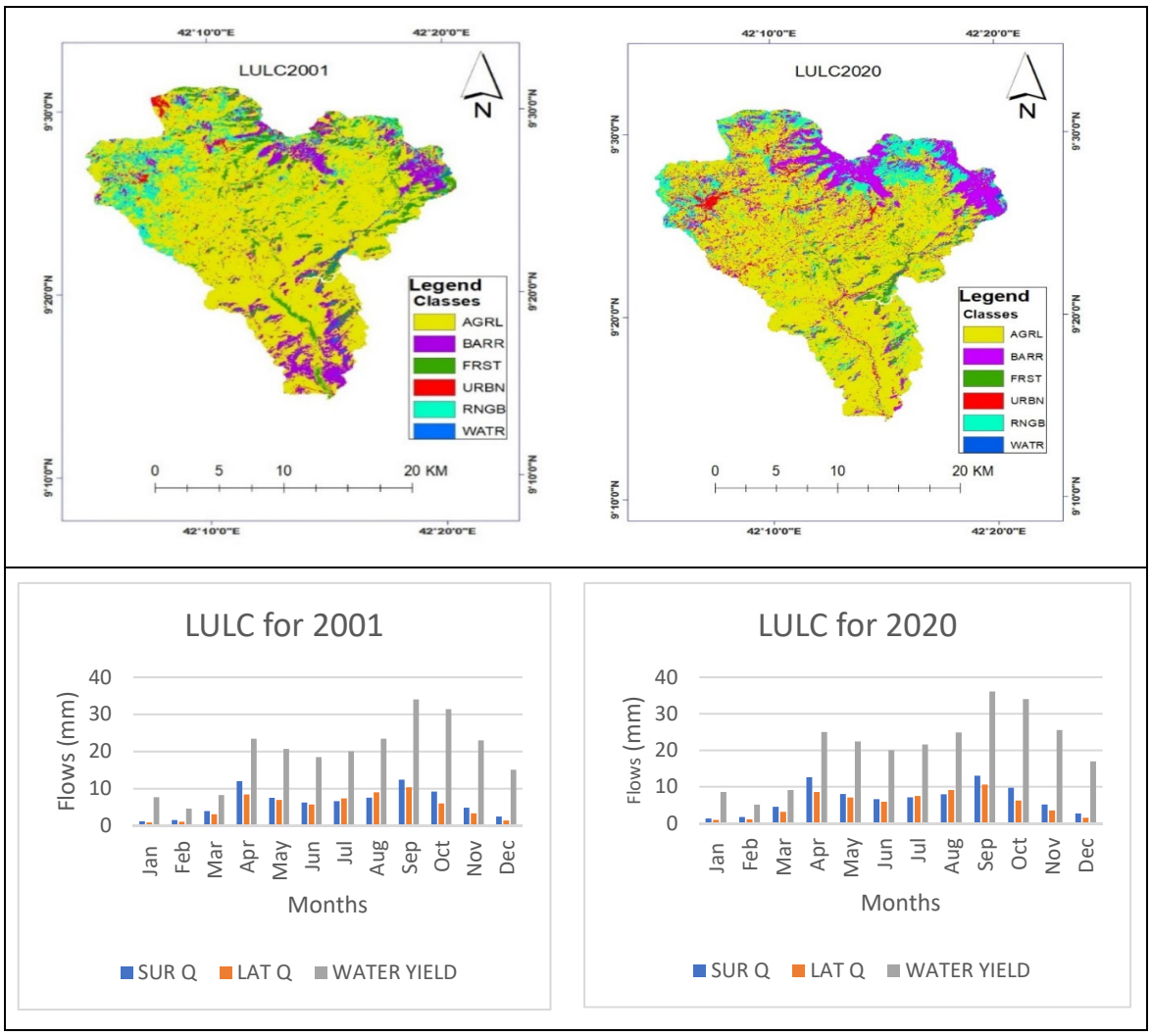

1. Introduction

Land use change is largely affected by the population growth [1,2]. The driving forces that affect hydrological conditions are land use land cover (LULC) changes and climate change [3]. Land use change has a vital role in disturbing the surface runoff and groundwater flow [4,5]. The Erer subbasin has a significant land use land cover change [6]. The study conducted in Upper Nile Basin indicated LULC change affected the surface runoff and evapotranspiration [7]. Similar studies indicated that the development of agricultural land, intensification of bare land, and urbanization resulted in stream flow increase [8,9]. In addition, the intensification of cropland and urbanization alters the soil moisture conditions and groundwater storage [10]. The LULC changes due to the loss of forest affects the infiltration rate season [9]. Settlement lands were the largest contributor to water yield [11].

The surface runoff and water yield were positively linked to variation in cropland and settlements. However, ground water flow and evapotranspiration were negatively linked to changes in cropland and settlement lands [12-15]. The increase in rainfall resulted in an increase in annual runoff [16]. Other study in Wabishebele Basin indicated portion of forest coverage and population concentration was found negatively correlated with surface runoff [17]. The output from similar study indicated that additional natural vegetation land changes to cropland or grazing lands, probably tends to decrease dry-season streams and exaggerate peak runoff [18]. The surface runoff extent has high positive correlation with cropland and population density and a strong negative correlation with natural vegetation [19,20]. Natural vegetation cover, expansion of agriculture and settlements were the main land use driver affecting the variation in hydrological components [21-25].

The LULC changes will have an impact on water resources [26]. Assessment of the hydrological impacts under LULC changes produced by different hydrological components [27]. Related studies will be used to understand the hydrological processes of water resource administration and development [28]. The continuous watershed situation assessment was vital for improved watershed management [8]. The LULC change effects analysis is the essential concern in watershed management at sub basin level [25]. This LULC change affects the hydrological cycle in complex ways with scale differences and different spatial-temporal scales under regional conditions [28]. To mitigate this problem now adays

there is high interest of using hydrological models in order to appropriately compute the diversified effects of a changing land use land cover [2].

The hydrologic models are likely to quantity and evaluate the quality of hydrological component. This hydrological component includes the amount of precipitation, actual evapotranspiration and water yield [27,29]. The interaction of land and water conservation practices were needed for the implementation of sustainable water resource management and planning under local and regional scale [9]. Sustainable water resource development was implemented by examining the land use land cover change effects on long-term changes in hydrological conditions and understanding the impacts of LULC change on hydrological components [3,10,18,30-32]. The soil and water assessment tool (SWAT] hydrological model was successfully simulated for water balance component analysis under the LULC change [3,33-35].

Defining the characteristics of hydrological circumstances regionally and locally is a challenge under LULC changes [36]. This is more severe in developing countries where there is a shortage of data, the degree of LULC change is indefinite [3]. For this reason, it is important to conduct studies about the land use/cover change effect, especially in watersheds with low hydrometeorological data availability such as the upper Erer sub basin. Determining the land use land cover changes and assessing their effects become particularly relevant for sustainable management of land and water resources in the long term for the study area. Various studies were analyzing the impact of LULC changes on the hydrological process; eg and others [37].

Researchers such as quantified the Impacts of Climate and Land Cover Changes on the Hydrological Regime of a Complex Dam Catchment Area, Pakistan [38]. Their findings indicated that the Complex Dam Catchment Area is expected to experience extreme hydrological events due to the land-use and climatic conditions of the river basin which focused on impacts on surface runoff. On the other hand, in Australia simulated hydrological responses to land-use change in the North Johnstone River catchment and found that land-use change impacted hydrological variables, with the most notable impact being on surface runoff [39]. Other study in Tanzania evaluated the land use land cover changes impacts of the Wami sub-basin considered only few hydrological parameters and suggested to include other hydrological parameters in order to better understand the hydrology of the basin for the optimal use of water resources [40].

Generally, despite their notable outputs, these and many other studies are limited to river sub-catchments/sub-basins using some or part of the hydrological components. Thus, they lack the ability to provide cumulative impacts of land use land cover changes (LULCCs) on the hydrology at local scale. Limited information is also available on the impact of land use and land cover change on soil and water resources in arid and semiarid areas of the country [41]. It is important to evaluate the land use land cover change impact, mainly at the local level [42]. Similarly, such problems are pertained in the Upper Erer subbasin, which has multiple land uses and considerable land use land cover changes [6]. Nevertheless, the increase in multiple LULCCs and their impacts, only few hydrological studies have been conducted on the region.

To understand challenges of the LULC changes effects in Ethiopia further studies are required to investigate the LUCC change impact on groundwater hydrology [41]. The current study has incorporated more hydrological components in the equation that represent a real situation of the catchment hydrology. This study objective is to assess the effects of LULC change on water balance, such as surface runoff, total water yield, groundwater flow, lateral flow, and evapotranspiration at subbasin scales using SWAT model. The study used for improved understanding of hydrological processes under changing LULC in the upper Erer subbasin.

2. Materials and Methods

2.1. Description of Study Area

The upper Erer subbasin, which is located physically in between 9o13'26.4" N to 9o31'26.4" N latitude and 42o4'40.8" E 42o20'38.4" E longitude found at the upper part of the Erer River Basin. The Erer River Basin is a tributary of Wabisheble Basin and found in the upper Wabishebele Basin, which drains from the Harar highlands. The Upper Erer Subbasin area is about 466.84 km2 with an elevation range from 1306 to 3019 meters as shown in (Figure 1). The Upper Erer River Alluvial Valley Plain is found about 10 to 20 km east and south east of Harar Town.

Ecologically, the upper Erer subbasin is categorized in to three climatic zones; Kolla (warm semiarid), varied from elevation 500 to 1500 meters, accounted for about 13.06 %, Woinadega (cool subhumid) varied from elevation 1500 to 2300 meters is accounted for 73.98 % and Dega (cool humid) varied from elevation 2300 to 3200 meters accounted for 12.97 % of the total drainage area [43]. The mean daily minimum and maximum temperatures were 12.78 and 26.72 °C respectively [44]. The regional agroecological zone climate highly dominated by Woinadega (cool subhumid). The population income mostly depends on agriculture [45].

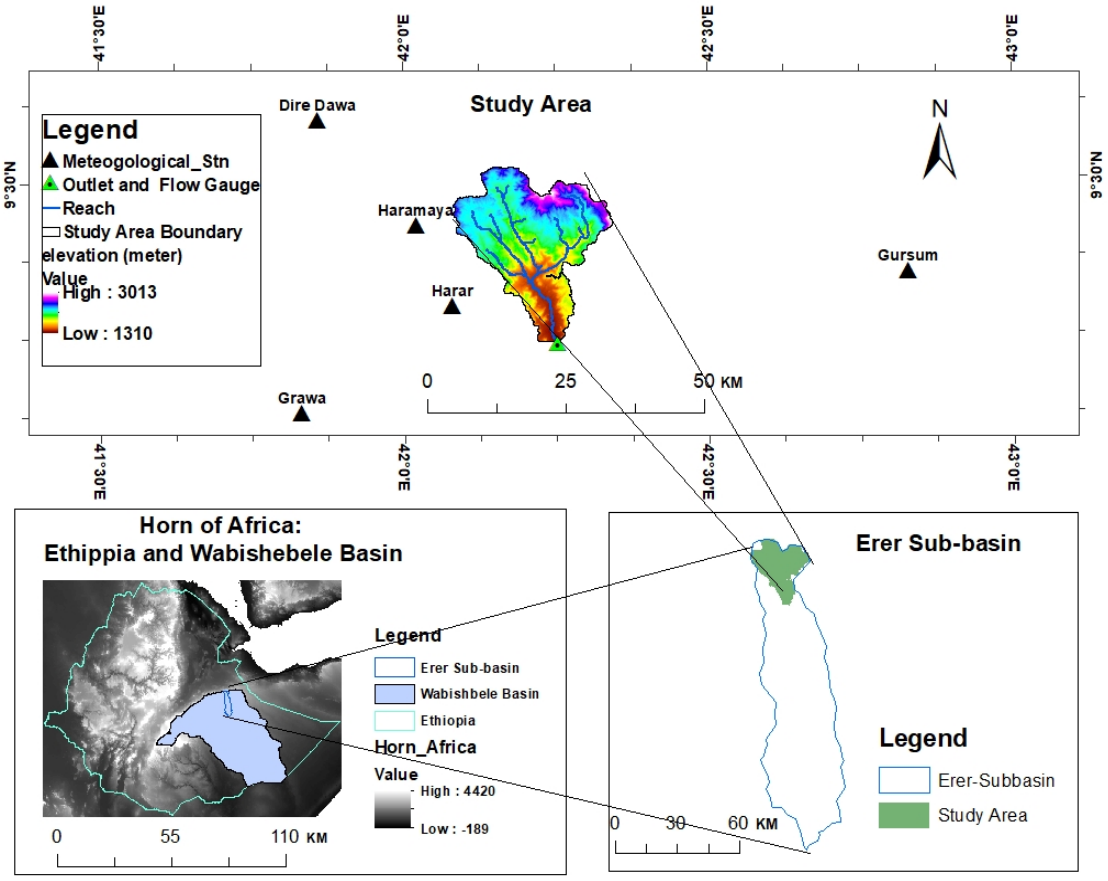

Figure 1: Study Area Location of the Upper Erer Subbasin

In this study SWAT hydrological model was employed for hydrological component assessment under LULC changes. Semi-distributed based modeling approaches are considered for a remote watershed that suffers from lack of continuous and good quality data [46]. The user identifies the type of projection and the projection settings within the interface when creating a new project [47]. The coordinate systems for running the model, and the projected coordinate systems like UTM (Universal Transverse Mercator) were used for this study using the appropriate UTM zone, WGS 84-UTM zone 37 N. The subbasins generated from the watershed were further divided into a hydrologic response unit (HRUs) in which each HRUs had exceptional soil–land use combinations. The hydrological cycle simulated by SWAT model is based on the water balance components indicated in Equation (1.1).

$$SW_t = SW_o + \sum_{i=1}^{t} (Pi - Qsurf - Ea - Wseep - Qgw) \ldots\ldots\ldots\ldots\ldots\ldots \text{Eq. 1.1}$$

where SW_t is the total soil water capacity (mm), SWo is the original soil water capacity (mm) at initial time i, t is the time in days, Pi is rainfall in mm/day, Qsurf is the surface flow in mm/day, Ea is evapotranspiration in mm/day, Wseep is the water percolation from the soil profile in mm/day, and Qgw is the groundwater recharge in mm/day.

In SWAT model simulation, the model computes evaporation from soil and plants separately. For this study, the Penman–Monteith potential evapotranspiration was selected and for runoff (rainfall-runoff) daily rainfall/CN/daily were selected for the watershed parameters for the assessment of water balance [48]. Soil Conservation Services (SCS) curve number method was chosen for surface runoff estimation [47]. In the SWAT model simulations various spatial and temporal data are required includes, Digital Elevation Model (DEM), soil map, meteorological data, land use land cover data. The DEM data with a grid resolution of 30 m by 30 m is downloaded from United States of Geological Survey (USGS) Earth Explorer website: (http://earthexplorer.usgs. gov/) https://vertex.daac.asf.alaska.edu/and used to generate the topography and slope of the sub-basin [49]. Using the DEM data, the SWAT model generates five slope categories. Soil data used for the study was generated from United Nations Food and Agriculture Organization (FAO) website and clipped by FAO soil map of Ethiopia collected from Ministry of Agriculture.

The FAO soil map of Ethiopia was prepared by the professionals considering the local circumstances of soil characteristics. SWAT soil map input data was prepared having soil map of the study area and lookup table. The soil map was linked to the model and used to indicate the soil type and the lookup table was used to describe the map using two columns arranged, one for the soil name and the other for soil values generated from the map [47]. In this study, the Map Windows in the MWSWAT database were used for the

soil database in Arc SWAT database to make compatible the user soil map data with the ARC SWAT database.

The temporal data used for SWAT model simulation are daily meteorological data. Both observed daily observed and global data (CFSR) are used for this study. The rainfall data was collected from ground rain gage observations from Dire Dawa, Girawa, Gursum, Haramaya, and Harar stations provided by the National Meteorological Institute of Ethiopia (NMIE) for the period (1979 to 2014). Whereas, others weather data (maximum and minimum temperatures, relative humidity, solar radiation and wind speed) were collected from Climate Forecasting System Reanalysis (CFSR) using the overlapping coordinate with the ground gauging stations [50-53].

Five meteorological ground stations were selected (Table) based on the quantity, quality, period, consistency, homogeneity, and their uniformity distribution around the Upper Erer subbasin. The missing data for the rainfall data were adjusted from the nearby stations using the arithmetic mean method and normal ratio method as recommended by [54]. The user weather databases were prepared and copied to the Arc SWAT database [47]. In this study, the user edited the entire user-wgn manually. Weather generator program, WGNmaker4.xlms was run to calculate the value of different precipitation parameters used for weather generator. This program uses the EXCEL macro to calculate the weather station statistics used for weather generator for SWAT model input. For RAINHHMX (*Maximum 0.5 hour rainfall in entire period of record for month*), if their values are not recorded locally, the value of 1/3 of the maximum daily rainfall of a month is taken cross ref: http://WWW-ssl.tamu.edu Texas A &M University [47,55].

Stations	Geographic position		Station topography (m)	Average yearly precipitation (mm)	Proportion of missing values (%)
	Latitude	Longitude			
Dire Dawa	9.60	41.86	1045	647	9.12
Haramaya	9.43	42.02	2025	816	12.92
Harar	9.30	42.08	1977	801	18.01
Girawa	9.13	41.83	2470	958	14.83
Gursum	9.35	42.39	1937	840	8.74

Table 1: Description of Gauging Stations and their Geographical Coordinates Including the Missing Values in %

The land use land cover data was prepared for SWAT input. The Image classification is conducted using ArcGIS interface under supervised image classification procedures to produce the LULC map. Image classification accuracy assessment was also used to check the accuracy for the land use land cover map generated from Landsat data. Detail image classification procedures were presented in the following sub-section. A lookup table that categorizes the unique land use code for the SWAT model were produced to link the grid values to SWAT LULC classes [47].

During the SWAT model processing the Hydraulic Response Units (HRUs) analysis was implemented by overlaying the classified LULC map, soil map, and slope map (generated from DEM). The overlay process was adjusted for specific percentage values of LULC (10%), soil (15%), and slope (15%) as recommended by [55].

2.2. Image Classification

For the extraction of LULC data, cloud-free (< 10%) dry season, and Land Sat images availability was considered for the periods. Seasonal differences in vegetation distribution were minimized using the same annual season as shown in Table 2. The Satellite images of the years 2001 (Landsat 7) and year 2020 (Landsat-8) were obtained from United States Geological Survey (USGS) (https://www.glovis.USGS.gov). The downloaded images were analyzed using ArcGIS and following the supervised classification approach to make a land cover map for the region [56].

Image classification accuracy assessment was used to detect the image classification accuracy for the classified LULC map generated from Land Sat data, and this was used to know the proximity of the images to the training sample on the classified images. Using the interactive supervised image classification, the LULC maps for 2001 and 2020 were produced. Due to a constraint of field data, Google Earth, a previously generated map of the region and the digitalized topographic map with 1:50,000 scale of 1st edition 2000 of Ethiopian Mapping Agency was used for the reference sample generation as suggested by [57]. The accuracy of the image classification was checked using the overall percentages of accuracy, user's accuracy, producer's accuracy, and the Kappa Coefficient [58,59]. The overall procedures were followed using the following equation described in Equation (1.2-1.5).

Reference data	Acquisition date Year/ Month /Day	Path/row	Image	Resolution
2001	2001/12/10	166/54	Landsat 7	30 x 30 m
2020	2020/12/22	166/54	Landsat 8	30 x 30 m

Table 2: Landsat Information for the Period under Consideration, Including the Acquisition Date, Path/ Row of Images, Image Types, and Image Resolution

$$\text{Overall accuracy} = \frac{\text{Total correctly classified pixels}}{\text{Total of classified pixels}} X100 \qquad \text{Equation (1.2)}$$

Where, total correctly classified pixels are the sum of major diagonal and total of classified sample points are the total number of reference samples points.

$$\text{Producer accuracy} = \frac{\text{Number of correctly classified pixels per class}}{\text{Number of reference totals per class}} X100 \quad \text{.....Equation (1.3)}$$

Where, the producer's accuracy indicates how well test set samples of the given cover type are classified.

$$\text{User accuracy} = \frac{\text{Number of correctly classified pixels per class}}{\text{Number of classified totals per class}} X100 \quad \text{.....Equation (1.4)}$$

Where, the user's accuracy is a measure of commission error that indicates the probability that a pixel classified into a given category actually represents that category on the ground.

$$\text{Kstat} = \frac{N\sum_{i=1}^{n} Sij - \sum_{i=1}^{n}(S_{Rtot} X S_{Ctot})}{N^2 - \sum_{i=1}^{n}(S_{Rtot} X S_{Ctot})} X100 \quad \text{.....Equation (1.5)}$$

Where Kstat is Kappa statistic coefficient, N is total number of samples, *Sij* is the product of total number of sample and total diagonal values, S_{Rtot} is row total, S_{Ctot} is the column total and n, is the number of categories. The coefficient evaluates the difference between the actual agreement of classified map and chance agreement of random classifier compared with reference data [59].

In this study, two approaches were followed for the model analysis between the periods; firstly, the LULC changes were analyzed and secondly, the anlysis of the LULC change effects on the hydrological components were evaluated. Figure 2 shows the detail process for the study analysis and output including supervised image classification using the ArcGIS for the land use land cover map preparation and impact study analysis using the Arc SWAT model.

2.3. Calibration and Validation

The SWAT model has calibrated and validated using stream flow used to compute the hydrologic components [48]. The SWAT model simulations using the measured flow were evaluated and well performed [8,10,11,16,26,60-63]. In addition to the automatic calibration, manual calibration has been adopted in different watersheds [64,65]. Manual calibration of SWAT is difficult in many large-scale applications. Nevertheless, the manual calibration process encourages the user to better understand the model and sensitive parameters [66]. The strengths of both the manual and autocalibration approaches can be used to facilitate the calibration process [67]. In this study, calibration and validation was performed both automatically and manually.

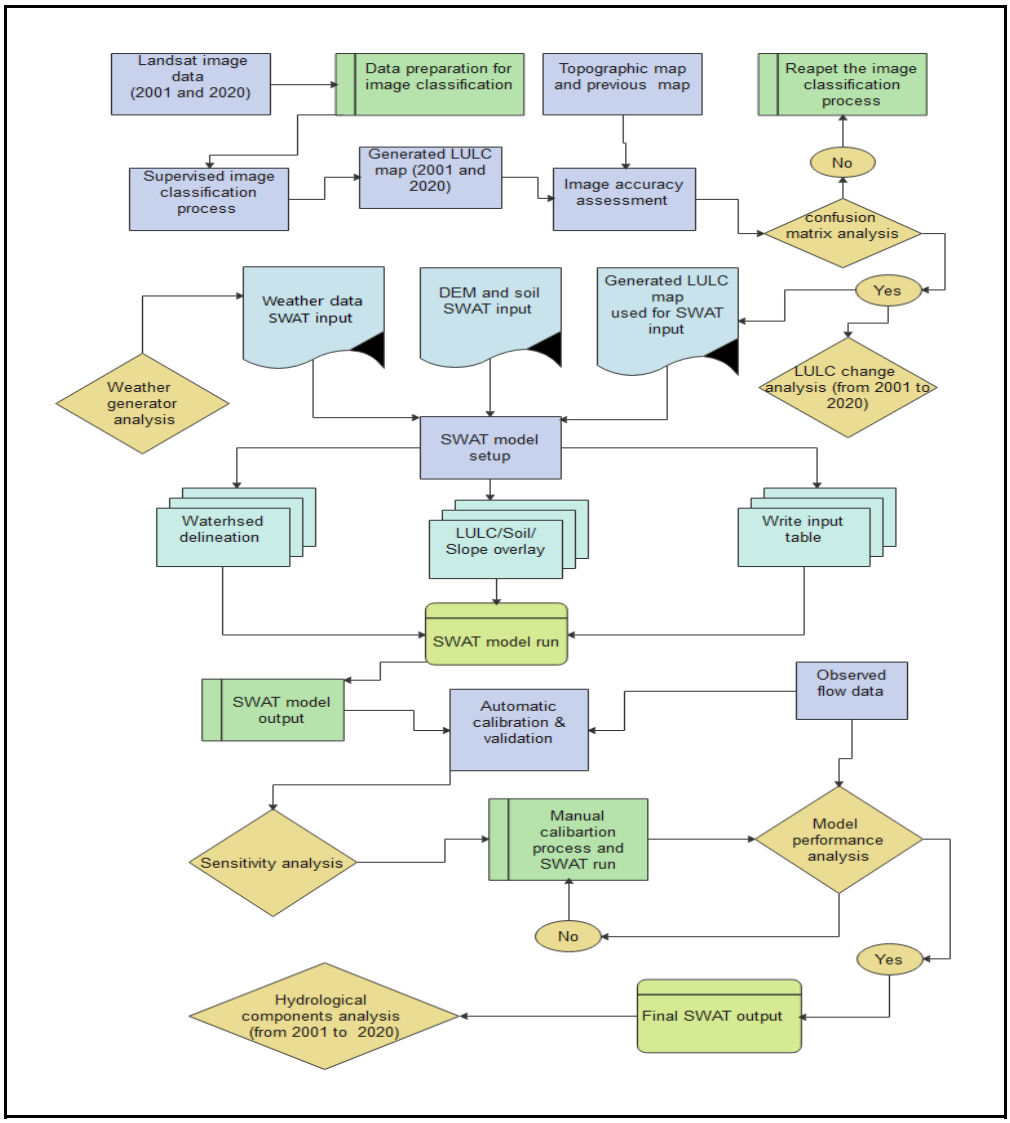

Figure 2: Conceptual Frame Work

More data were important for a reliable model calibration at the watershed scale [26,54]. After the ARCSWAT model simulation is completed, the calibration was performed both automatically and manually [66,68]. Monthly streamflow flow data at the outlet of the upper Erer subbasin is showed in (Figure 1) for the periods (1984-1990) and (1993-1996) were provided by the Ministry of Water and Energy of Ethiopia (MWEE). Mmodel calibration and validation were performed using recorded daily stream flow data at Upper Erer River outlet of hydrological stations provided by the Ministry of Water and Energy of Ethiopia (MWEE). Hence, the daily flow data were changed to monthly flow data and arranged according to the SWAT-CUP input data format requirement for model calibration and validation. To execute calibration and validation processes, SUFI-2 (sequential uncertainty fitting) algorithm in SWAT-CUP2012 were used to identify sensitive parameters form selected parameters. SWAT-CUP is an auto-calibration and uncertainty analysis tool with four built-in analysis algorithms [69].

The SWAT model simulation is run for period (1979-2014) as a monthly basis and the SWATCUP model is used to identify sensitive parameters. Autocalibration approach was used to assess the sensitive parameters and know the range of parameter values. The manual calibration/ validation involves varying the input parameter values within the recommended ranges to produce simulated flow data that were analyzed with the measured flow data [70].

2.4. Sensitivity Analysis and SWAT Model Performance Evaluation

The parameter sensitivity analysis helps to detect the most influential flow parameters that are used for calibration and validation in the model [71]. The sensitivity analysis was performed using the SWAT-Calibration and Uncertainty Procedure (SWAT-CUP) [72]. SUFI-2 is an iterative procedure that were used for model calibration and validation to attain a reasonable result [10,71,73]. The model was run using the best parameter output values and measure the model performance using the simulated and observed streamflow data using performance measures such as; Nash-Sutcliffe coefficient (NS), coefficient of determination (R2), and percent bias (PBIAS). The performance measures of NSE, R2 and PBIAS were calculated using Equations (1.6, 1.7 and 1.8), respectively.

$$NSE = 1 - \left[\frac{\sum_{i=1}^{n}(Q_{oi} - Q_{si})^2}{\sum_{i=1}^{n}(Q_{oi} - \text{Qoav})^2}\right] \quad \text{Equation (1.6)}$$

$$R^2 = 1 - \left[\frac{\sum_{i=1}^{n}(Q_{oi} - Q_{sav})(Q_{oi} - Q_{oav})}{\sum_{i=1}^{n}(Q_{si} - Q_{sav})^2 \sum_{i=1}^{n}(Q_{oi} - Q_{oav})^2}\right] \quad \text{Equation (1.7)}$$

$$PBIAS = 1 - \left[\frac{\sum_{i=1}^{n}(Q_{oi} - Q_{si})}{\sum_{i=1}^{n}(Q_{oi})}\right] \quad \text{Equation (1.8)}$$

Where; Q_{oi} and Q_{si}: the observed and simulated streamflow data, Q_{oav} and Q_{sav} the average of the observed and simulated stream flow data. The model evaluation performance rankings were established for each recommended statistical value.

2.5. Land use Change Analysis for Hydrological Response

The land use change affected the water balance components [15,22,74]. For this study to assess the water balance components of the land cover change effects. The LULC maps for the period of 2001 and 2020 with the same climatic data were used for the model analysis. The changes in hydrological component results were assessed from the effects of the LULC change on the hydrologic response in the watershed.

3. Results and Discussions

3.1. Image Classification Accuracy Analysis

Using supervised/maximum likelihood classification the land cover classes were generated applying training samples developed from ground truth reference sample data by employing Google Earth, previously generated map of the region, and topographic maps. The random reference sample points for the years 2001 and 2020 were 129 and 143, respectively. A matrix was generated using the reference samples along the rows with the classified images along the columns were compared to identify the relation. About six LULC classes were generated for the study area such as: agricultural land, bare land, forest land, settlements, shrub lands, and water bodies.

After land cover classes were generated, the LULC maps of 2001 and 2020 were prepared. Comparison was made using the sample LULC classes of the classified layer and the reference layer. Then, the classification accuracy of the resulting LULC maps was assessed. To analyze the accuracy of LULC maps, overall, producer's accuracy, user's accuracy and Kappa coefficient were computed using Equations (1.2, 1.3, 1.4 and 1.5), respectively. Table 3 and Table 4 shows the overall accuracy, producer's accuracy, user's accuracy, and kappa coefficient values for the reference years. The overall accuracy for the years 2001 and 2020 was greater than the minimum value (85 %) recommended by [75]. For the years 2001 and 2020, the kappa coefficient was 0.84 and 0.89, respectively. The Kappa coefficient was greater than 0.81 as per suggested by, which implies the agreements are strong agreement [76].

The producer's accuracy for the years 2001 and 2020 for the settlement (URBN) land cover is 78.6 and 85.7 %, respectively. This imply the producer's accuracy assessment for settlement land cover is less than the others land cover. Similarly, the producer's accuracy for water body land cover for the year 2001 is 80 %. The user's accuracy for water bodies (WATR) for the year 2001 is 80%. The user's accuracy for the year 2020 is.7% for the shrub lands (RNGB) cover class which is the smallest value.

Matrix	AGRL	BARR	FRST	URBN	RNGB	WATR	Sum References	User's Accuracy
AGRL	35	2	0	1	2	0	**40**	87.5
BARR	0	12	0	1	0	0	**13**	92.3
FRST	5	0	22	0	0	2	**29**	75.9
URBN	0	0	0	11	0	0	**11**	100.0
RNGB	0	0	0	1	25	0	**26**	96.2
WATR	0	0	2	0	0	8	**10**	80.0
Sum Classified	**40**	**14**	**24**	**14**	**27**	**10**	**129**	
Producer's Accuracy	87.5	85.7	91.7	78.6	92.6	80.0		

Table 3: Image Classification Accuracy Assessment for year 2001 (Overall Accuracy= 87.6%, Kappa Coefficient=0.84)

Matrix	AGRL	BARR	FRST	URBN	RNGB	WATR	Sum References	User's Accuracy
AGRL	40	2	0	0	1	0	**43**	93.0
BARR	1	15	0	1	0	0	**17**	88.2
FRST	0	0	26	0	0	0	**26**	100.0
URBN	0	0	0	18	0	0	**18**	100.0
RNGB	4	0	0	2	16	2	**24**	66.7
WATR	0	0	0	0	0	15	**15**	100.0
Sum Classified	**45**	**17**	**26**	**21**	**17**	**17**	**143**	
Producer's Accuracy	88.9	88.2	100.0	85.7	94.1	88.2		

Table 4: Image Classification Accuracy Assessment for Year 2020 (Overall Accuracy= 90.91%, Kappa Coefficient=0.89)

3.2. Changes in Land use Land Cover Analysis

Based on the image classification processing, six land cover classes were generated in this study area. The areal coverage and land cover change for the years 2001 and 2020 of LULC classifications are showed in Table 5 Figure 3 shows the spatial distribution LULC for the years 2001 and 2020. The result indicated that forest lands were significantly decreased from 2001 to 2020 by about 18.6 km2, followed by agricultural land (18.5 km2) and water bodies (2.8 km2). But bare land, shrub land, and settlements were increased histrionically by 14.9, 14.3, and 10.8 km2, respectively from years 2001 to 2020. The forest land was decreased and the urban land was increased. This were confirmed by similar studies [63,77]. From Figure 3, the bare lands were intensified at the southern part and at the edge of the watershed outlet. The shrub lands were increased at the expense of agricultural land and forest land. The new shrub lands were occupied from years 2001 to 2020. This was probably due to high plantation of chat crop in the region, which is considered as shrub land. About 17.12 % of the total LULU type were transformed during the years from 2001 to 2020.

Shrub land, bare land, and settlements had increased from years 2001 to 2020. In contrast, forest land was decreased, perhaps as a result of growth in population and urbanization, this agrees with the study on the upper Genale River Basin [58]. The LULC map demonstrated the agricultural land was the major LULC class, shrub lands and bare lands were the second and third dominant coverage in the study area, respectively in Table 5. The forest land and water body showed a reduction and bare land and urban areas have increased, this agreed with the study done on Erer sub watershed [6]. But this output was disagreed with other study conducted on the Koga Watershed that indicated croplands were intensified [78].

Table 6 shows the comparison matrix for the LULC changes. The comparison matrix revealed that the maximum changes in the LULC change were for forest and water body comparison and the minimum changes were detected for settlement and shrub land comparison. The change in LULC for agricultural and forest land comparison was nearly 1, this implies the change is comparable.

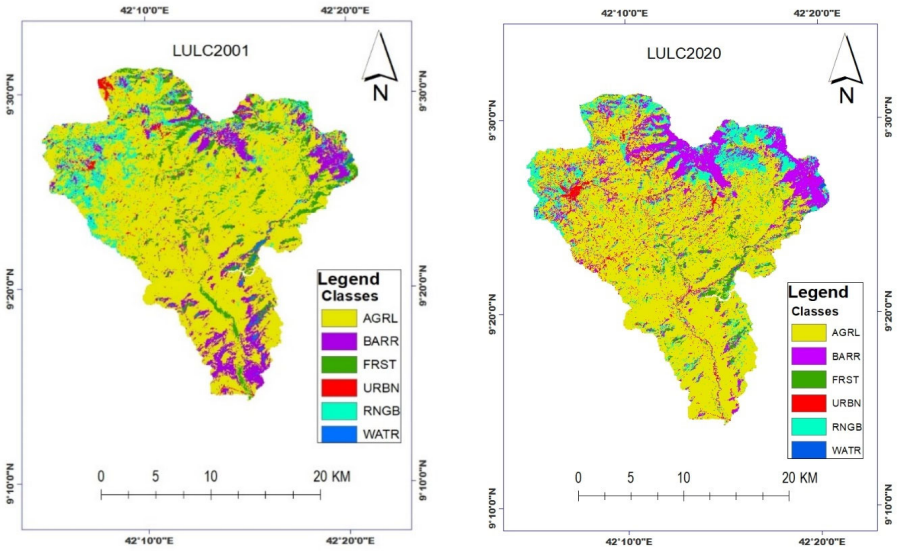

Figure 3: LULC Maps for the Years 2001 and 2020

3.3. Watershed Delineation and HRU Analysis

The watershed delineation was generated using the raster mask of the study area, DEM map, and upper Erer subbasin outlet. At this position there was an installed hydrometric gauging instrument. The delineation process generates around 23 subbasins and 146 Hydraulic Response Units (HRUs) as showed in Figure 4.

Land use Type	2001 LULC		2020 LULC		LULC changes	
	Area coverage		Area coverage		Area coverage changes	
	km2	%	km2	%	km2	%
AGRL	327.0	70.04	308.4	66.07	-18.5	-3.97
BARR	53.0	11.34	67.9	14.53	14.9	3.19
FRST	36.0	7.71	17.3	3.71	-18.6	-3.99
URBN	6.9	1.47	17.6	3.78	10.8	2.30
RNGB	40.4	8.66	54.8	11.73	14.3	3.07
WATR	3.6	0.78	0.8	0.18	-2.8	-0.60
TOTAL	466.8	100	466.8	100		

Table 5: LULC Change Analysis from Years 2001 to 2020 (km2 Denotes the Area in Square Kilometers)

Figure 5 shown the soil and slope classification map. This indicated that the Dystric Cambisols were mostly found at the higher elevation of the watershed. The Eutric Nitosols were found at the lower elevation of the watershed with most of the slope class range 8 to 15 %. The soil data in the Upper Erer sub catchment were shown in Table 7. The major soil types in the region, namely: Dystric Cambisol, Eutric Nitosols, and Humic Cambisols. In the region, the land use land cover was classified in to six classes, namely: bare land, cropland, forestland, settlements, shrublands, and water body. In the region, the cropland covers the highest areas and the water body covers the minimum area [6].

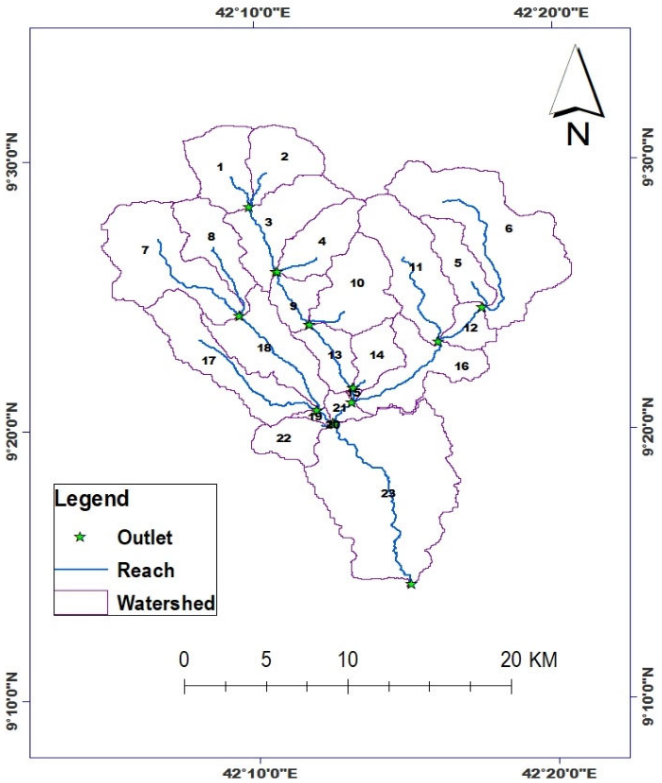

Figure 4: Upper Error Subbasin Delineation Output

Citation: Mummed, B. A., Seleshi, Y. (2025). Assessment of the Effects of Land use Land Cover Change on Water Balance Components in the Upper Erer Subbasin, Wabishebele Basin, Ethiopia. *J Earth Environ Waste Manag, 3*(1), 1-20.

Matrix	AGRL	BARR	FRST	URBN	RNGB	WATR
AGRL	1	1.24	0.99	1.72	1.72	6.62
BARR		1	0.80	1.38	1.04	5.32
FRST			1	1.73	1.73	6.66
URBN				1	0.75	3.84
RNGB					1	5.12
WATR						1

Table 6: Land use Land Cover Change Analysis Matrix for the Years 2001 to 2020

Soil features	Description soil map of the world (1974)	SWAT Soil Codes
Soil features	Dystric Cambisols	Bd30-2-3c-9
	Humic Cambisols	Bh12-3c-31
	Eutric Nitosols	Ne15-3c-159

Table 7: Description of Soil Class and Soil-Code for SWAT Model Input for the Region

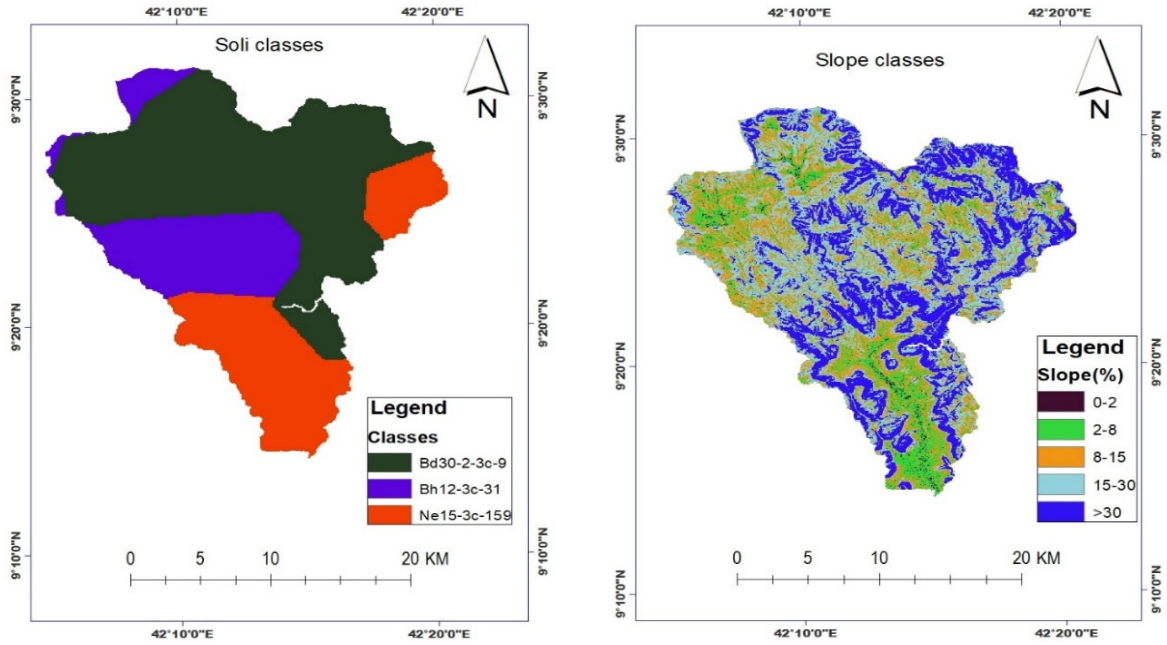

Figure 5: Soil and Slope Classes for the Study Area

In the classification processes, six major LULC classes were generated [6]. The LULC class description was taken from [48]. Table 8 shows the SWAT code used to link the LULC map to the SWAT land use database.

Value/ class	Original/ Map LULC Name	SWAT Description CROP NAME	SWAT CODE CPNM
1	Agricultural Lands	Agricultural land -generic	AGRL
2	Barren Lands	Barren	BARR
3	Forest Lands	Forest Mixed	FRST
4	Settlements	Residential	URBN
5	Shrub Lands	Range Brush	RNGB
6	Water Bodies	Water Body	WATR

Table 8: Description of LULC Classification and LULC Code for SWAT Model

The prepared LULC, soil and slope maps have been systematically overlayed to get the HRU analysis results for the watershed. The maximum soil groups in the watershed were the Dystric Cambisol covering around 54.53 %, the Eutric Nitosols with an area coverage for 25.09 % and Humic Cambisol covering around 20.38% of the watershed.

The maximum coverage slope class of 15 to 30% covers around 34.21 % of the watershed area, and the smallest coverage is 1.09 % with the slope class of less than 2 % slope. From the results, more than 70 % of the slope coverages were concentrated within the range of 2 to 30 % slope class and more than 62.6 % slope coverage were > 15 % slope class. This result was confirmed by [17].

3.4. Sensitivity Analysis and Model Performance Evaluation

Studies done globally rank the sensitive parameters such as showed CN2 (Initial soil conservation service (SCS) curve number), ALPHA_BF (Baseflow alpha factor), GW_DELAY (Groundwater delay), and GWQMN.gw (Threshold depth of water in the shallow aquifer for return flow to occur) have high sensitivity values [27]. Other study showed that parameters like: CN, ALPHA_BF, and GW_DELAY were more sensitive [9]. Other study conducted on tropical watershed indicated CN2, GW_REVAP (Groundwater "revap" coefficient) and SOL AWC (Soil water available capacity) were more sensitive [73]. While, other studies indicated three sensitive parameters such as: CN2, GW_DELAY, and SOL_K (1) (Saturated hydraulic conductivity of first soil layer) [47,63]. Other scholar identified the influential parameters includes; surface runoff (CN2) and total flow parameters (SOL_AWC, ESCO (Soil evaporation compensation factor)) [66]. Meanwhile, other study showed CN2, SURLAG (Surface runoff lag time), and CANMX (Maximum canopy storage) were the most three sensitive parameters [10].

Sensitive parameters	References
ESCO, CN2, ALPHA_BF, REVAPMN, SOL_AWC, GW_REVAP, CH_K2, and GWQMN	[61]
CN2, ESCO, SOL_AWC, SOL_Z, ALPHA_BF, ALPHA_BF, CH_K2, CH_K2, REVAPMN, and GWQMIN	[79]
CN2, SOL_AWC, SOL_Z and REVAPMN	[80]
CN2, GW_REVAP.gw, RCHRG_DP.gw, SOL_AWC (1).sol, GW_DELAY.gw, ESCO.hru, SURLAG.bsn, REVAPMN.gs and GWQMN.gw	[47]
CN2.mgt, _SOL_AWC (...).sol, RCHRG_DP.gw, CH_K2.rte, GW_DELAY.gw ALPHA_BF.gw, SLSUBBSN.hru, GW_REVAP.gw, EPCO.bsn, SOL_K (...).sol and HRU_SLP.hru	[56]
Alpha_Bf, Cn2, Esco, Gw_Delay, Gwqmn, Revapmin, Rchrg_DP, Sol_Awc, Sol_K, and Surlag	[81]
RCHRG_DP, SOL_K, CN2, GWQMN, ESCO, SLSUBBSN, GW_REVAP, SOL_AWC and ALPHA_BF	[82]

Table 9: Literature Survey of the Most Sensitive Parameters in Some Related Studies in Ethiopia

Among the sensitive parameters identified in various studies above CN2 parameter implied rapid changes in land use classes [79-83]. Understanding this sensitive parameter help to reduce the calibration iteration process [31]. The ranges of parameter value were adapted from the SWAT manual [48]. Identification of the most influential parameters form different literature used to easily understand the mostly used parameters and Table 9 shows the literature summary for the most influential parameters in Ethiopia. Using this step about17 parameters were identified during the first autocalibration process. Using the sensitivity analysis of sufi2 algorithm in the SWATCUP model, out of the 17 selected parameters, the most influential 10 parameters in the region were identified. Figure 6 shows the sensitive parameters values from the autocalibration analysis using SWAT-cup of sufi2.

The identifier in Figure 6, (R__) state of the relative change in the parameter to the value from the SWAT database was multiplied by (1 + a given value), (V__) refers the parameter value from the SWAT database was changed by the given value and (A_) refers the value was added to the current parameter value. In this model, for spatial parameters (eg. CN2, hydraulic conductivity, bulk density, and others), we use (r_) or (a_) before the parameters of the model to modify the existing values (SWAT output) with new values (fitted values) by modification. But, for non -spatial parameters, we use (v_) to modify the existing values to the new values by replacement.

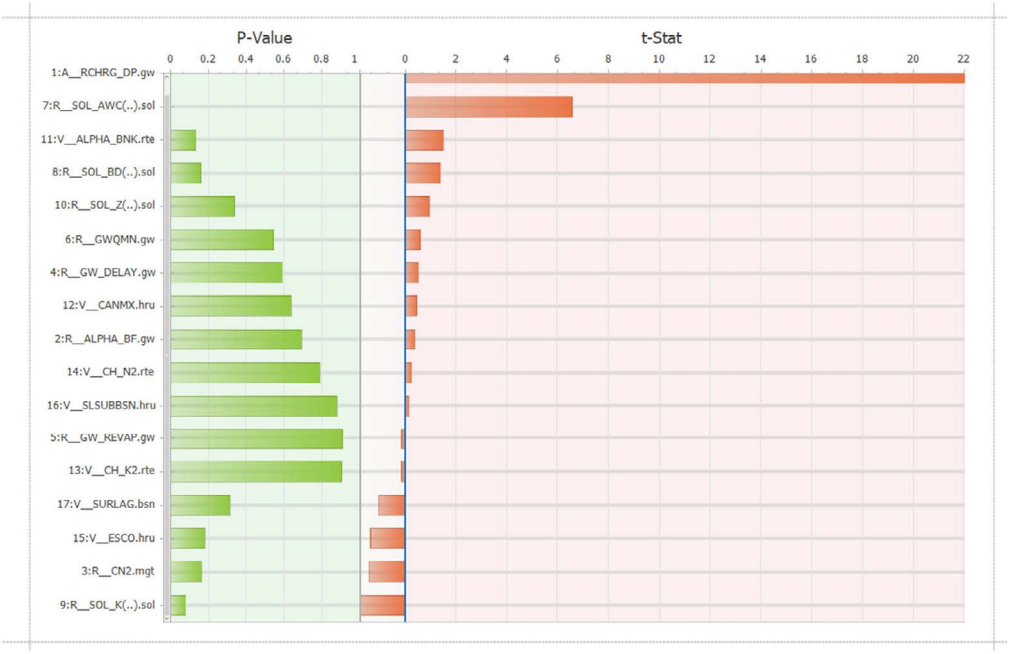

Figure 6: Global Sensitivity Analysis Results of Parameters

The smaller absolute p-value and the larger absolute t-value were considered and ten sensitive parameters were identified from seventeen parameters selected from the literature survey (Figure 6). From the result, the most sensitive parameters were CN2, SOL_AWC, ESCO, GWQMN, and others. This agreed with most studies in Ethiopia [9,27,47,61,84]. The model performance is also checked with manual calibration procedures using the SWAT model manual helper; repetitive simulation (twenty-eight) was carried out during the process by adjusting the surface runoff and groundwater flow sensitive parameters. The final influential parameters and their fitted values were shown in Table 10. The four parameters; CN2, SOL_K, GWQMN, and REVAPMN were identified as the most influential parameters out of 10 parameters selected from autocalibration process.

Parameter Name	Description (unit)	Default values	Final fitted values	Min. range	Max. range
CN2.mgt	Initial soil conservation service (SCS) curve (none)	65	72.5	35	98
SOL_AWC (1).sol	Soil water available capacity (mm H2O/mm soil)	0.092	0.097	0	1
SOL_K (1).sol	Saturated hydraulic conductivity (mm/hr)	7.04	21.12	0	200
ESCO.hru	Soil evaporation compensation factor (none)	0.95	0.92	0.01	1
EPCO.hru	Plant uptake compensation factor (none)	1	0.98	0	1
GWQMN.gw	Threshold water level in shallow aquifer for baseflow (mm)	1000	1300	0	5000
REVAPMN.gw	Threshold depth of water in the shallow aquifer for “revap” to occur (mm)	750	75	0	500
GW_REVAP.gw	Groundwater ‘revap’ coefficient (none)	0.02	0.018	0.02	0.2
SURLAG.bsn	Surface runoff lag coefficient (none)	4	2.5	0.05	24
RCHRG_DP.gw	deep aquifer percolation fraction (none)	0.05	0.042	0	1

Table 10: Sensitive Parameter Description and their Values (Default, Fitted, Minimum and Maximum Ranges). The Abbreviations Min. and Max. Denotes the Minimum and Maximum Ranges, Respectively.

3.5. Model Simulation

Automatic and manual calibration procedures were used. The manual procedures suggested by were used to modify the SWAT model parameters [48]. The manual calibration and validation were done by adjusting the sensitive parameters that were identified from autocalibration for groundwater parameters and surface runoff parameters. The flow calibration procedures suggested by were implemented. The model simulation was performed for period (1979-2014) using three years warmup period (1979-1981) [65]. The calibration and validation process taken place using observed monthly streamflow data for calibration period (1984–1990) and validation period (1993–1996). In the initial SWAT model simulation, the base flow was too low and the evaporation was too high, adjustments were made on the groundwater flow evaporation parameters; by decreasing GWQMN and GW-REVAP and increasing REVAPMN parameters repetitively until the model performance measures such as coefficient of determination (R^2), Nash–Sutcliffe efficiency (NSE), and percent of bias (PBIAS).

Then, the baseflow became too high, and the peak flows were too low, adjustments were made to the surface runoff and baseflow parameters by increasing CN2 and decreasing the other flow parameters like; SURLAG, ESCO, EPCO. Finally, the same adjustments were made to the soil parameters (SOL_K (1), SOL_AWC (1)) until the statistical measures reaching acceptable values [67,72]. The final SWAT model simulation output was found to be checked and performance parameters for calibration period were R^2 (0.84), NSE (0.65) and PBIAS (-23.04). Similar procedures were followed using the flow data for validation period found that the performance measures were R^2 (0.83), NSE (0.53) and PBIAS (-14.16). The result indicated that the model performance measures were in acceptable range for NSE > 0.50 and R2 > 0.70, and if PBIAS ± 25% [85,86].

During the manual calibration, the process has in the order of sensitivity and influence on the flow parameters for runoff and groundwater. First, the CN2 was calibrated and then the GW_REVAP, REVAPMN, and RCHRG_DP in the order of sensitivity of the parameters need adjustment [67]. The calibration and validation include all kinds of climate situations; like dry years, wet years, and moderate occur in both periods [85-88]. SWAT output values were checked as per the SWAT developers' suggestions and all output values for model performance were within the satisfactory range of PBIAS ≤ (±25%), R^2 > 0.7 and NSE > 0.5 suggested by [85,65]. This agreed with a similar study on Gilgel Gibe watershed [89]. Similarly, the results agreed with the study on Angreb watershed [77].

From the result, model performance values, R2 values higher than 0.83 for both the calibration and validation periods as suggested by, this indicates that there is a strong agreement between the simulation and measured data [24]. This study result of the performance measure; PBIAS was difference with the study on hangar catchment of PBAIS which is less than 10% [47]. For this study, R^2 value was higher and NSE value was smaller than a similar study on Bilate catchment [63]. In general, the performance indicator values found for the model simulation showed a very good performance rate in simulating the SWAT models as suggested by [47]. The simulated and measured monthly flow correlation diagram indicating the coefficients of determination (R^2) for calibration was 0.84 and for validation was 0.83 as shown in Figure 7.

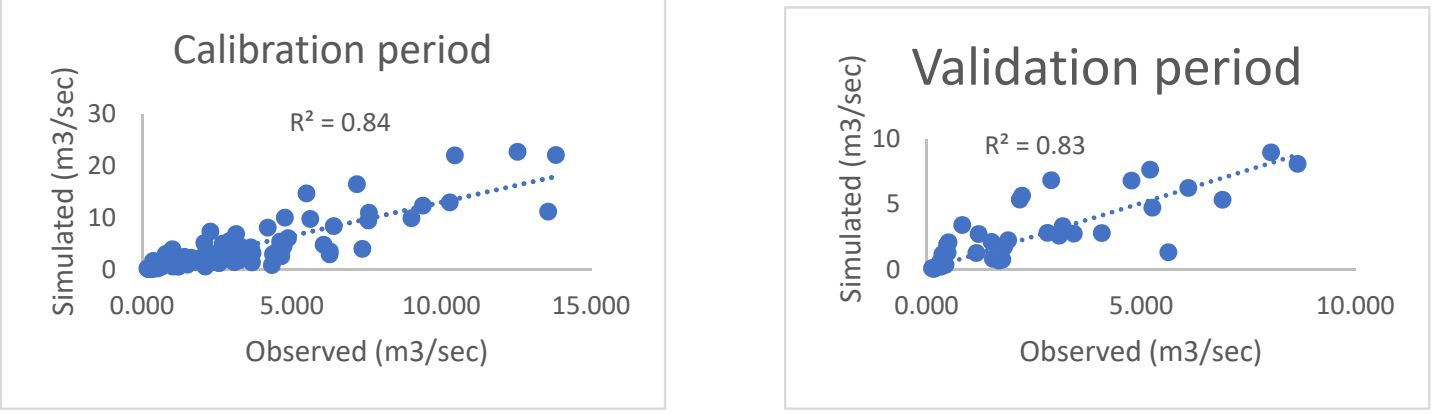

Figure 7: Scatter Plot of Observed and Simulated Monthly Streamflow for the Study Area.

The monthly steam flow hydrographs for the model simulation were shown in Figure 8. The results showed that the model has overestimated the flow for July 1986 and September 1986 and under estimated flows for August 1989, September 1989, and August 1994.

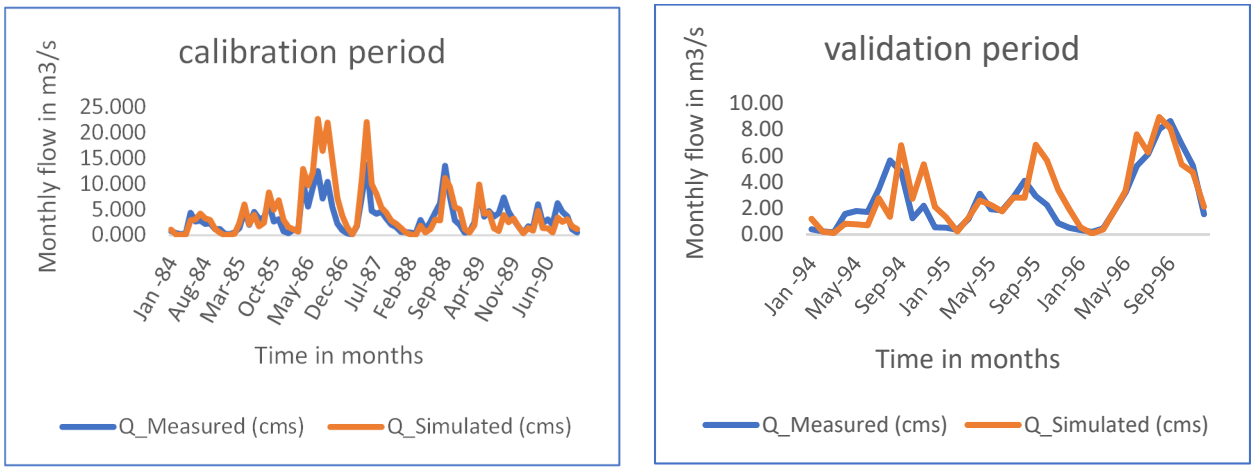

Figure 8: Monthly Stream Flow Hydrograph for Calibration and Validation

3.6. Effects of Land use Land Cover Change on Hydrological Response

The hydrological response effect due to land use land cover change for the years 2001 and 2020 were presented in Table 11. The groundwater flow increases by 10.39%, water yields by 8.22 %, surface runoff by 6.03% and lateral flow by 1.85% only. Whereas, evapotranspiration shows decrease by 3.34 % from 2001 to 2020. This was confirmed by a study on tropical catchments [90]. The result indicated there was high evapotranspiration with low runoff in the region. Hydrological responses were varied due to the effects of the LULC changes in the region [68]. In this study, the decrease in forested land led to a reduced in infiltration rate, this was probably due to the reduction in surface roughness and reduction in average annual evapotranspiration, and this agreed with the study on the East African watershed [32]. In the region, there was an increase in settlement lands and a decrease in natural forest, this contributed high surface runoff as confirmed by similar studies in other parts of Ethiopia [6,57]. From the results, the evapotranspiration was decreased due to a shortage of soil moisture as a result of the decrease in natural vegetation cover [7]. Other study supporting the findings of this study revealed that the conversion of forest land to shrubs and settlements leads to a reduction in evapotranspiration and an increase in surface runoff [88]. The surface runoff increased by 6.03 %, this finding was supported by other study conducted on Tekeze dam [8].

The water yield was also increased in this study, and this agreed with the similar study [91]. The surface runoff was increased due the expansion of settlement lands and the expense of other land covers [34]. Other study supporting this study findings indicated that an increase in water yields and decrease in evapotranspiration due to the reduction and forest lands and tends to soil moisture decrease soil [11]. Generally, the changes in surface runoff result from the conversion of natural vegetation to other lands as suggested in similar study [10,31,83]. Overall, the results showed that about 68 and 65.2 % of the precipitation were lost to evapotranspiration for the years 2001 and 2020, respectively. Whereas, about 27.2 and 29.5 % of the total precipitation were only changed to water yields in 2001 and 2020, respectively. From these results, the reduction in evapotranspiration was possibly related to the decrease in forest coverage. The groundwater consumption from precipitation were 15.3 % for the year 2001 and 16.95 % for the year 2020. This was probably due the natural vegetation land was reduced and the shrub lands were increased.

Hydrological response	LULC changes		Parameter increase/ decrease	
	LULC 2001	LULC 2020	Amount	%
Surface runoff (mm)	75.82	80.39	4.57	6.03
Groundwater flow (mm)	129.68	143.16	13.48	10.39
Evapotranspiration (mm)	574.2	555	-19.20	-3.34
Lateral flow (mm)	63.85	65.03	1.18	1.85
Water yields (mm)	230.25	249.18	18.93	8.22
Precipitation (mm)	844.4	844.4	-	-

Table 11: Hydrological Response of Mean Annual Land use, Land Cover Change

Figure 9 shown the temporal distribution of water balance components in the study area. From the results, the main rainy seasons from April to May and June to September were the maximum mean monthly surface runoff and water yields. However, October, November, December, and January were dry months with low surface runoff and water yields in the region [56,92].

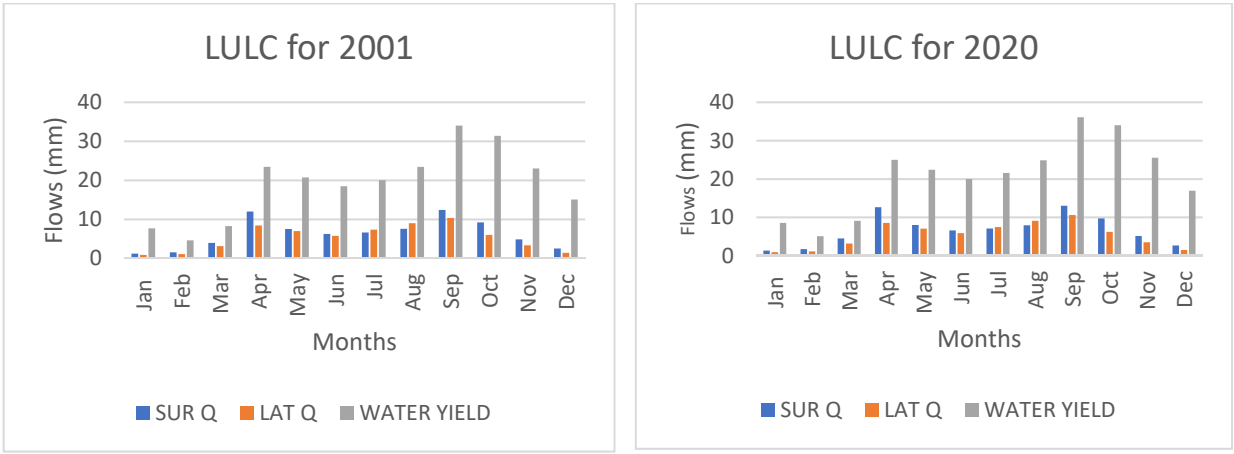

Figure 9: Average Monthly Distribution of Hydrological Response

4. Conclusions

This study was focused to assess the LULC change and their effects to the hydrological response from the years 2001 to 2020. In the watershed delineation process, around 23 subbasins and 146 HRUs were generated in the study sub basin. The HRUs were generated from the overlay analysis of HRUs analysis using the Arc SWAT interface of LULC, soil and slope maps of the watershed. Three soil types, namely: Dystric Cambisol, Eutric Nitosols, and Humic Cambisol and five slope categories were generated from the analysis.

The CN2, ESCO, SOL_AWC, and REVAPMN identified as the most influential parameters in the sub-basin that affect the flow. The LULC change assessment for the years 2001 to 2020 revealed the agricultural lands were reduced by 18.5 km2, water bodies by 2.8 km2, and forest lands by 18.6. However, shrub lands were increased by 14.3 km2. The bare lands and settlements were increased by 14.9 km2 and 10.8 km2, respectively. These were probably agricultural and forest lands were changed to shrub land and/ or settlements and/ or bare land. The shrub lands were the maximum coverage increment next to bare land. This is due to the intensification of the Chat crop in the region were most of the agricultural and other lands were changed to this crop.

Under the LULC changes, the hydraulic responses effects for the sub-basin were evaluated from the years 2001 to 2020. The output showed that the surface runoff, ground water flow, and water yields were increased by 6.03, 10.39, and 8.22 % from 2001 to 2020, respectively. The evapotranspiration was decreased by 3.34 %, these were due to the decrease of the natural vegetation.

The SWAT model simulation showed that the model well performed for the assessments of LULC changes in the upper Erer subbasin. Nevertheless, the hydro-meteorological data inadequacy and quality in the region indicated the satellite data involvement in the future to better understand the local conditions under changing situations. Even if the study of LULC change on the hydrological components are insufficient in the subbasin level but, slightly serves policy makers and stake holders for better utilization of natural resources and proposed management practices for future analysis. Moreover, the manual calibration approach for the SWAT model assistances the user for improved knowledge and understanding the hydrological parameters. Future studies may need the integration of manual and automatic calibration approaches for the upper Erer subbasin by using refined hydrometeorological data for the improved output. Though, the LULC on hydrological process shows a considerable change in streamflow and overall hydrological responses, the study has not covered the sediment yield analysis that possibly affected by the LULC types. Future studies may consider the sediment yield in the subbasin including other parameters (such as; climate change) that affect the hydrological response in the region.

Acknowledgments

Acknowledgements were to the National Meteorological Institute and the Ministry of Water and Energy of Ethiopia, Ministry of Agriculture of Ethiopia for providing data.

Funding

This research received no external funding.

References

1. Arnold, J. G., & Allen, P. M. (1999). Automated methods for estimating baseflow and ground water recharge from streamflow records 1. *JAWRA Journal of the American Water Resources Association, 35*(2), 411-424.
2. Tufa, D. F., Abbulu, Y. E. R. R. A. M. S. E. T. T. Y., & Srinivasarao, G. V. R. (2014). Watershed hydrological response to changes in land use/land covers patterns of river basin: A review. *International Journal of Civil, Structural, Environmental and Infrastructure Engineering Research and Development (IJCSEIERD), 4*(2), 157-170.
3. Torabi Haghighi, A., Darabi, H., Shahedi, K., Solaimani, K., & Kløve, B. (2020). A scenario-based approach for assessing the hydrological impacts of land use and climate change in the Marboreh Watershed, Iran. *Environmental Modeling & Assessment, 25*(1), 41-57.
4. Napoli, M., Massetti, L., & Orlandini, S. (2017). Hydrological response to land use and climate changes in a rural hilly basin in Italy. *Catena, 157,* 1-11.

5. Pandey, B. K., Khare, D., Kawasaki, A., & Meshesha, T. W. (2021). Integrated approach to simulate hydrological responses to land use dynamics and climate change scenarios employing scoring method in upper Narmada basin, India. *Journal of Hydrology, 598*, 126429.
6. Weldu Woldemariam, G., & Edo Harka, A. (2020). Effect of land use and land cover change on soil erosion in erer sub-basin, Northeast Wabi Shebelle Basin, Ethiopia. *Land, 9*(4), 111.
7. Berihun, M. L., Tsunekawa, A., Haregeweyn, N., Meshesha, D. T., Adgo, E., et al. (2019). Hydrological responses to land use/land cover change and climate variability in contrasting agro-ecological environments of the Upper Blue Nile basin, Ethiopia. *Science of the Total Environment, 689*, 347-365.
8. Welde, K., & Gebremariam, B. (2017). Effect of land use land cover dynamics on hydrological response of watershed: Case study of Tekeze Dam watershed, northern Ethiopia. *International Soil and Water Conservation Research, 5*(1), 1-16.
9. Belihu, M., Tekleab, S., Abate, B., & Bewket, W. (2020). Hydrologic response to land use land cover change in the Upper Gidabo Watershed, Rift Valley Lakes Basin, Ethiopia. *HydroResearch, 3*, 85-94.
10. Galata, A. W., Demissei, T. A., & Leta, M. K. (2020). Watershed hydrological responses to changes in land use and land cover at Hangar Watershed, Ethiopia. Iranica Journal of Energy & Environment, 11(1), 1-7.
11. Lu, Z., Zou, S., Qin, Z., Yang, Y., Xiao, H., et al. (2015). Hydrologic responses to land use change in the loess plateau: case study in the Upper Fenhe River Watershed. *Advances in Meteorology, 2015*(1), 676030.
12. Aragaw, H. M., Goel, M. K., & Mishra, S. K. (2021). Hydrological responses to human-induced land use/land cover changes in the Gidabo River basin, Ethiopia. *Hydrological Sciences Journal, 66*(4), 640-655.
13. Quilbé, R., Rousseau, A. N., Moquet, J. S., Savary, S., Ricard, S., et al. (2008). Hydrological responses of a watershed to historical land use evolution and future land use scenarios under climate change conditions. *Hydrology and Earth System Sciences, 12*(1), 101-110.
14. Chemura, A., Rwasoka, D., Mutanga, O., Dube, T., & Mushore, T. (2020). The impact of land-use/land cover changes on water balance of the heterogeneous Buzi sub-catchment, Zimbabwe. *Remote Sensing Applications: Society and Environment, 18,* 100292.
15. Gyamfi, C., Ndambuki, J. M., & Salim, R. W. (2016). Hydrological responses to land use/cover changes in the Olifants Basin, South Africa. *Water, 8*(12), 588.
16. Daba, M. H. (2010). *Sensitivity of SWAT Simulated Runoff to Temperature and Rainfall in the Upper Awash Sab-Basin, Ethiopia. Hydrol Current Res 9: 293. doi: 10.4172/2157-7587.1000293 Page 2 of 7 Volume 9• Issue 1• 1000293 Hydrol Current Res, an open access journal ISSN: 2157-7587 The daily weather data required to run the SWAT hydrological model were acquired from the National Meteorology Agency (NMA). The daily data for maximum and minimum temperature, rainfall, relative humidity, and wind speed were obtained* (Doctoral dissertation, These data cover a period of 30 years from 1980 to).
17. Wudineh, F. A., Moges, S. A., & Kidanewold, B. B. (2021). Flood change detection and attribution using simulation approach in data-scarce watersheds: A case of Wabi Shebele river basin, Ethiopia. *Journal of Water Resource and Protection, 13*(5), 362-393.
18. Mango, L. M., Melesse, A. M., McClain, M. E., Gann, D., & Setegn, S. (2011). Land use and climate change impacts on the hydrology of the upper Mara River Basin, Kenya: results of a modeling study to support better resource management. *Hydrology and earth system sciences, 15*(7), 2245-2258.
19. Ochoa-Tocachi, B. F., Buytaert, W., De Bievre, B., Célleri, R., Crespo, P., et al. (2016). Impacts of land use on the hydrological response of tropical Andean catchments. *Hydrological Processes, 30*(22), 4074-4089.
20. Wudineh, F. A., Moges, S. A., & Kidanewold, B. B. (2022). Flood generation mechanisms and potential drivers of flood in Wabi-Shebele River basin, Ethiopia. *Natural Resources, 13*(1), 38-51.
21. Gebremicael, T. G., Mohamed, Y. A., & Van der Zaag, P. (2019). Attributing the hydrological impact of different land use types and their long-term dynamics through combining parsimonious hydrological modelling, alteration analysis and PLSR analysis. *Science of the Total Environment, 660,* 1155-1167.
22. Marhaento, H., Booij, M. J., & Hoekstra, A. Y. (2018). Hydrological response to future land-use change and climate change in a tropical catchment. *Hydrological sciences journal, 63*(9), 1368-1385.
23. Nyssen, J., Clymans, W., Descheemaeker, K., Poesen, J., Vandecasteele, I., et al. (2010). Impact of soil and water conservation measures on catchment hydrological response—a case in north Ethiopia. *Hydrological processes, 24*(13), 1880-1895.
24. Kenea, U., Adeba, D., Regasa, M. S., & Nones, M. (2021). Hydrological responses to land use land cover changes in the Fincha'a Watershed, Ethiopia. *Land, 10*(9), 916.
25. Wu, F., Zhan, J., Su, H., Yan, H., & Ma, E. (2015). Scenario-Based Impact Assessment of Land Use/Cover and Climate Changes on Watershed Hydrology in Heihe River Basin of Northwest China. *Advances in Meteorology, 2015*(1), 410198.
26. Koycegiz, C., & Buyukyildiz, M. (2019). Calibration of SWAT and two data-driven models for a data-scarce mountainous headwater in semi-arid Konya closed basin. *Water, 11*(1), 147.
27. Gebre, S. L., Getahun, D., Fufa, F., Diriba, O. H., & Alemayehu, E. (2022). Hydrological responses of land use land cover change on the Hangar catchment, Blue Nile Basin. *Ethiopian Journal of Applied Science and Technology, 13*(1), 33-44.
28. Ding, Y., Feng, H., & Zou, B. (2022). Remote Sensing-Based Estimation on Hydrological Response to Land Use and Cover Change. *Forests, 13*(11), 1749.
29. Takala, W., Adugna, T., & Tamam, D. (2016). The effects of land use land cover change on hydrological process of Gilgel Gibe, Omo Gibe Basin, Ethiopia. *Int. J. Sci. Eng. Res, 7*(8), 117-128.
30. Mahmoud, S. H., & Alazba, A. A. (2015). Hydrological response to land cover changes and human activities in

arid regions using a geographic information system and remote sensing. *Plos one, 10*(4), e0125805.
31. Ankita, D. P., & Kazuo, N. (2014). Modeling hydrological response to land use change in watersheds of viti levu island, FIJI. *Journal of Environmental Research and Development, 8*(3), 492.
32. Baker, T. J., & Miller, S. N. (2013). Using the Soil and Water Assessment Tool (SWAT) to assess land use impact on water resources in an East African watershed. *Journal of hydrology, 486*, 100-111.
33. Mohammad, M. E., Al-Ansari, N., & Knutsson, S. (2016). Application of SWAT model to estimate the annual runoff and sediment of Duhok reservoir watershed. In *8th International Conference on Scour and Erosion-Oxford, Uk< 12-15 September 2016* (pp. 1129-1136). Taylor & Francis Group.
34. Getu Engida, T., Nigussie, T. A., Aneseyee, A. B., & Barnabas, J. (2021). Land use/land cover change impact on hydrological process in the Upper Baro Basin, Ethiopia. *Applied and Environmental Soil Science, 2021*(1), 6617541.
35. Abbaspour, K. C., Vejdani, M., Haghighat, S., & Yang, J. (2007, December). *SWAT-CUP calibration and uncertainty programs for SWAT. In MODSIM 2007 international congress on modelling and simulation, modelling and simulation society of Australia and New Zealand* (pp. 1596-1602). Dübendorf, Switzerland: Swiss Federal Institute of Aquatic Science and Technology.
36. Aredo, M. R., Hatiye, S. D., & Pingale, S. M. (2021). Impact of land use/land cover change on stream flow in the Shaya catchment of Ethiopia using the MIKE SHE model. *Arabian Journal of Geosciences, 14*(2), 114.
37. Moreira, L. L., Schwamback, D., & Rigo, D. (2018). Sensitivity analysis of the Soil and Water Assessment Tools (SWAT) model in streamflow modeling in a rural river basin. *Revista Ambiente & Água, 13*(6), e2221.
38. Masood, M. U., Haider, S., Rashid, M., Aldlemy, M. S., Pande, C. B., et al. (2023). Quantifying the impacts of climate and land cover changes on the hydrological regime of a complex dam catchment area. *Sustainability, 15*(21), 15223.
39. Zhang, Y., You, Q., Chen, C., & Ge, J. (2016). Impacts of climate change on streamflows under RCP scenarios: A case study in Xin River Basin, China. *Atmospheric research, 178,* 521-534.
40. Ngondo, J., Mango, J., Nobert, J., Dubi, A., Li, X., et al. (2022). Hydrological response of the Wami–Ruvu basin to land-use and land-cover changes and its impacts for the future. *Water, 14*(2), 184.
41. Negese, A. (2021). Impacts of land use and land cover change on soil erosion and hydrological responses in Ethiopia. *Applied and Environmental Soil Science, 2021*(1), 6669438.
42. Taye, M. T., Willems, P., & Block, P. (2015). Implications of climate change on hydrological extremes in the Blue Nile basin: a review. *Journal of Hydrology: Regional Studies, 4,* 280-293.
43. ABABA, A. (1998). Agro-ecological Zones of Ethiopia.
44. National Meteorological Agency (NMA). Mean Monthly Rainfall Data; NMA: Addis Ababa, Ethiopia, 2015.
45. Mihertu, Y. F. (2019). Over View of Socio Economic Data on Eastern Ethiopia Region (Harar Biodiversity Center Working Zone). *Acta Scientific Agriculture, 3,* 196-206.
46. Addis, H. K., Strohmeier, S., Ziadat, F., Melaku, N. D., & Klik, A. (2016). Modeling streamflow and sediment using SWAT in Ethiopian Highlands. *International Journal of Agricultural and Biological Engineering, 9*(5), 51-66.
47. Winchell, M., Srinivasan, R., Di Luzio, M., & Arnold, J. (2013). ArcSWAT interface for SWAT2012: user's guide. *Blackland Research Center, Texas AgriLife Research, College Station, 1*-464.
48. Arnold, J. G., Kiniry, J. R., Srinivasan, R., Williams, J. R., Haney, E. B., & Neitsch, S. L. (2011). *Soil and water assessment tool input/output file documentation version 2009.* Texas Water Resources Institute.
49. Her, Y., Frankenberger, J., Chaubey, I., & Srinivasan, R. (2015). Threshold effects in HRU definition ofthe soil and water assessment tool. *Transactions of the ASABE, 58*(2), 367-378.
50. Nkiaka, E., Nawaz, N. R., & Lovett, J. C. (2017). Evaluating global reanalysis datasets as input for hydrological modelling in the Sudano-Sahel region. *Hydrology, 4*(1), 13.
51. Dile, Y. T., & Srinivasan, R. (2014). Evaluation of CFSR climate data for hydrologic prediction in data-scarce watersheds: an application in the Blue Nile River Basin. *JAWRA Journal of the American Water Resources Association, 50*(5), 1226-1241.
52. NCEI 2020 Climate Forecasting System (CRFS). National Centers for Environmental Information (National Centers and Atmospheric Administration-NCDC). Available from: https://www.ncdc.noaa.gov/data-access/model-data/model-datasets/climate-forecast-systemversion2-cfsv2.
53. Saha, S., Moorthi, S., Wu, X., Wang, J., Nadiga, S., et al. (2014). The NCEP climate forecast system version 2. *Journal of climate, 27*(6), 2185-2208.
54. Egigu, M. (2020). Techniques of filling missing values of daily and monthly rain fall data: a review. *SF J. Environ. Earth Sci, 3*(1).
55. Winchell, M., Srinivasan, R., Di Luzio, M., & Arnold, J. (2013). ArcSWAT interface for SWAT2012: user's guide. *Blackland Research Center, Texas AgriLife Research, College Station, 1*-464.
56. Shanko, D., & Camberlin, P. (1998). The effects of the Southwest Indian Ocean tropical cyclones on Ethiopian drought. *International Journal of Climatology: A Journal of the Royal Meteorological Society, 18*(12), 1373-1388.
57. Shigute, M., Alamirew, T., Abebe, A., Ndehedehe, C. E., & Kassahun, H. T. (2022). Understanding hydrological processes under land use land cover change in the upper Genale River Basin, Ethiopia. *Water, 14*(23), 3881.
58. Mir, S. A., Mattoo, D., Bhat, M. S., & Maheen, M. M. (2022). Dynamics of land-use/land cover changes in upper Jhelum catchment of Kashmir Himalayas, India. *Indian Journal of Ecology, 49*(5), 1634-1641.
59. Lillesand, T.M.; Kiefer, R.W.; Chipman, J.W. Remote Sensing and Image Interpretation, 7th ed.; Wiley: New York, NY, USA, 2015, ISBN 9781118343289.
60. Kuma, H. G., Feyessa, F. F., & Demissie, T. A. (2021).

Hydrologic responses to climate and land-use/land-cover changes in the Bilate catchment, Southern Ethiopia. *Journal of Water and Climate Change, 12*(8), 3750-3769.

61. Setegn, S. G., Srinivasan, R., & Dargahi, B. (2008). Hydrological modelling in the Lake Tana Basin, Ethiopia using SWAT model. *The Open Hydrology Journal, 2*(1).
62. Ngondo, J., Mango, J., Nobert, J., Dubi, A., Li, X., et al. (2022). Hydrological response of the Wami–Ruvu basin to land-use and land-cover changes and its impacts for the future. *Water, 14*(2), 184.
63. Leta, M. K., Demissie, T. A., & Tränckner, J. (2021). Hydrological responses of watershed to historical and future land use land cover change dynamics of Nashe watershed, Ethiopia. *Water, 13*(17), 2372.
64. Santhi, C., Arnold, J. G., Williams, J. R., Dugas, W. A., Srinivasan, R., et al. (2001). Validation of the swat model on a large rwer basin with point and nonpoint sources 1. *JAWRA Journal of the American Water Resources Association, 37*(5), 1169-1188.
65. Neitsch, S. L. (2005). Soil and water assessment tool theoretical documentation version 2005/Grassland. *Soil and Water Research Laboratory, Agricultural Research Service, Blackland Research Center, Texas Agricultural Experiment Station.*
66. Arnold, J. G., Moriasi, D. N., Gassman, P. W., Abbaspour, K. C., White, M. J., Srinivasan, R., ... & Jha, M. K. (2012). SWAT: Model use, calibration, and validation. *Transactions of the ASABE, 55*(4), 1491-1508.
67. Van Liew, M. W., Arnold, J. G., & Bosch, D. D. (2005). Problems and potential of autocalibrating a hydrologic model. *Transactions of the ASAE, 48*(3), 1025-1040.
68. Nobert, J., & Jeremiah, J. (2012). Hydrological response of watershed systems to land use/cover change. a case of Wami River Basin. *The Open Hydrology Journal, 6*(1).
69. Abbaspour, K. C., Yang, J., Maximov, I., Siber, R., Bogner, K., et al. (2007). Modelling hydrology and water quality in the pre-alpine/alpine Thur watershed using SWAT. *Journal of hydrology, 333*(2-4), 413-430.
70. Balascio, C. C., Palmeri, D. J., & Gao, H. (1998). Use of a genetic algorithm and multi-objective programming for calibration of a hydrologic model. *Transactions of the ASAE, 41*(3), 615-619.
71. Abbaspour, K. C., Vaghefi, S. A., & Srinivasan, R. (2017). A guideline for successful calibration and uncertainty analysis for soil and water assessment: a review of papers from the 2016 international SWAT conference. *Water, 10*(1), 6.
72. Abbaspour, K. C. (2015). SWAT calibration and uncertainty programs. *A user manual, 103,* 17-66.
73. Roth, V., Nigussie, T. K., & Lemann, T. (2016). Model parameter transfer for streamflow and sediment loss prediction with SWAT in a tropical watershed. *Environmental Earth Sciences, 75*(19), 1321.
74. Koch, F. J., Van Griensven, A., Uhlenbrook, S., Tekleab, S., & Teferi, E. (2012). The Effects of land use change on hydrological responses in the choke mountain range (Ethiopia)-a new approach addressing land use dynamics in the model SWAT.
75. Anderson, J. R. (1976). *A land use and land cover classification system for use with remote sensor data* (Vol. 964). US Government Printing Office.
76. Viera, A. J., & Garrett, J. M. (2005). Understanding interobserver agreement: the kappa statistic. *Fam med, 37*(5), 360-363.
77. Getachew, H. E., & Melesse, A. M. (2012). The impact of land use change on the hydrology of the Angereb Watershed, Ethiopia. *International Journal of Water Sciences, 1*(6).
78. Ayele, H. A., Aga, A. O., Belayneh, L., & Wanjala, T. W. (2023). Hydrological responses to land use/land cover changes in Koga watershed, upper Blue Nile, Ethiopia. *Geographies, 3*(1), 60-81.
79. Assfaw, A. T. (2019). Calibration, validation and performance evaluation of SWAT model for sediment yield modelling in Megech reservoir catchment, Ethiopia. *Journal of Environmental Geography, 12*(3-4), 21-31.
80. Mekonnen, M. A., Wörman, A., Dargahi, B., & Gebeyehu, A. (2009). Hydrological modelling of Ethiopian catchments using limited data. *Hydrological Processes: An International Journal, 23*(23), 3401-3408.
81. Shawul, A. A., Alamirew, T., & Dinka, M. O. (2013). Calibration and validation of SWAT model and estimation of water balance components of Shaya mountainous watershed, Southeastern Ethiopia. *Hydrology and Earth System Sciences Discussions, 10*(11), 13955-13978.
82. Desta, H., & Lemma, B. (2017). SWAT based hydrological assessment and characterization of Lake Ziway sub-watersheds, Ethiopia. *Journal of Hydrology: Regional Studies, 13,* 122-137.
83. Singh, L., & Saravanan, S. (2020). Simulation of monthly streamflow using the SWAT model of the Ib River watershed, India. *HydroResearch, 3,* 95-105.
84. Abbaspour, K. C., Rouholahnejad, E., Vaghefi, S. R. I. N. I. V. A. S. A. N. B., Srinivasan, R., Yang, H., et al. (2015). A continental-scale hydrology and water quality model for Europe: Calibration and uncertainty of a high-resolution large-scale SWAT model. *Journal of hydrology, 524,* 733-752.
85. Moriasi, D. N., Arnold, J. G., Van Liew, M. W., Bingner, R. L., Harmel, R. D., et al. (2007). Model evaluation guidelines for systematic quantification of accuracy in watershed simulations. *Transactions of the ASABE, 50*(3), 885-900.
86. Moriasi, D. N., Gitau, M. W., Pai, N., & Daggupati, P. (2015). Hydrologic and water quality models: Performance measures and evaluation criteria. *Transactions of the ASABE, 58*(6), 1763-1785.
87. Faramarzi, M., Srinivasan, R., Iravani, M., Bladon, K. D., Abbaspour, K. C., et al. (2015). Setting up a hydrological model of Alberta: Data discrimination analyses prior to calibration. *Environmental Modelling & Software, 74*, 48-65.
88. Gan, T. Y., Dlamini, E. M., & Biftu, G. F. (1997). Effects of model complexity and structure, data quality, and objective functions on hydrologic modeling. *Journal of hydrology, 192*(1-4), 81-103.
89. Warburton, M. L., Schulze, R. E., & Jewitt, G. P. (2012). Hydrological impacts of land use change in three diverse

South African catchments. *Journal of Hydrology, 414*, 118-135.

90. Naha, S., Rico-Ramirez, M. A., & Rosolem, R. (2021). Quantifying the impacts of land cover change on hydrological responses in the Mahanadi river basin in India. *Hydrology and Earth System Sciences, 25*(12), 6339-6357.
91. Bessah, E., Raji, A. O., Taiwo, O. J., Agodzo, S. K., Ololade, O. O., et al. (2020). Hydrological responses to climate and land use changes: The paradox of regional and local climate effect in the Pra River Basin of Ghana. *Journal of Hydrology: Regional Studies, 27*, 100654.
92. Cook, K. H., & Vizy, E. K. (2013). Projected changes in East African rainy seasons. *Journal of Climate, 26*(16), 5931-5948.